

## Supporting Information

### Quinoline-based tetrazolium prochelators: formazan release, iron sequestration, and antiproliferative efficacy in cancer cells

Yu-Shien Sung and Elisa Tomat

Department of Chemistry and Biochemistry, The University of Arizona, 1306 E. University Blvd., Tucson AZ 85721-0041 (USA).

E-mail: tomat@arizona.edu

#### Table of Contents

	page
1. Materials and methods .....	S2
2. Synthesis of formazan compounds.....	S2
3. Iron-binding tests in buffered aqueous solutions of formazan compounds .....	S4
4. Synthesis and structural characterization of Fe(QF-H) <sub>2</sub> .....	S5
5. Synthesis of tetrazolium compounds.....	S9
6. Solution properties of tetrazolium compounds .....	S11
7. Cell-based assays and biological characterization .....	S13
8. References .....	S19
9. NMR Spectra ( <sup>1</sup> H and <sup>13</sup> C).....	S20

## 1. Materials and methods

Unless stated otherwise, all chemicals were purchased from commercial suppliers and used as received. All reactions were carried out under atmospheric pressure. Aluminum-backed silica gel plates (thickness: 200  $\mu\text{m}$ ) were used to monitor reactions by thin layer chromatography (TLC). Chromatographic purifications on silica gel were conducted on a Biotage Isolera One Flash instrument. NMR spectra were recorded using a Bruker AVIII-400 or a Bruker NEO-500 instrument at the University of Arizona Department of Chemistry and Biochemistry NMR Facility (RRID:SCR\_012716).  $^1\text{H}$  and  $^{13}\text{C}\{^1\text{H}\}$  NMR spectra were referenced internally to residual solvent peaks in  $\text{CDCl}_3$  ( $^1\text{H}$  7.26;  $^{13}\text{C}$  77.0),  $\text{DMSO-}d_6$  ( $^1\text{H}$  2.50;  $^{13}\text{C}$  39.5),  $\text{CD}_3\text{OD}$  ( $^1\text{H}$  3.31;  $^{13}\text{C}$  49.0), or  $\text{CD}_2\text{Cl}_2$  ( $^1\text{H}$  5.32;  $^{13}\text{C}$  53.8). All mass spectrometry data were obtained at University of Arizona Analytical & Biological Mass Spectrometry Facility (RRID:SCR\_023370). Elemental analyses were performed by Numega Resonance Laboratories (San Diego, CA).

UV-visible absorption spectra were acquired using Agilent Cary 60 spectrophotometers at ambient temperature. Reverse-phase HPLC analyses were carried out on an Agilent Infinity II system with a ZORBAX Eclipse XDB-C18 column (80  $\text{\AA}$ , 4.60 x 250 mm, 5  $\mu\text{m}$ , 1 mL/min flow rate). Cyclic voltammograms were collected with a Gamry Reference 600 potentiostat employing a single-compartment cell and a three-electrode setup.

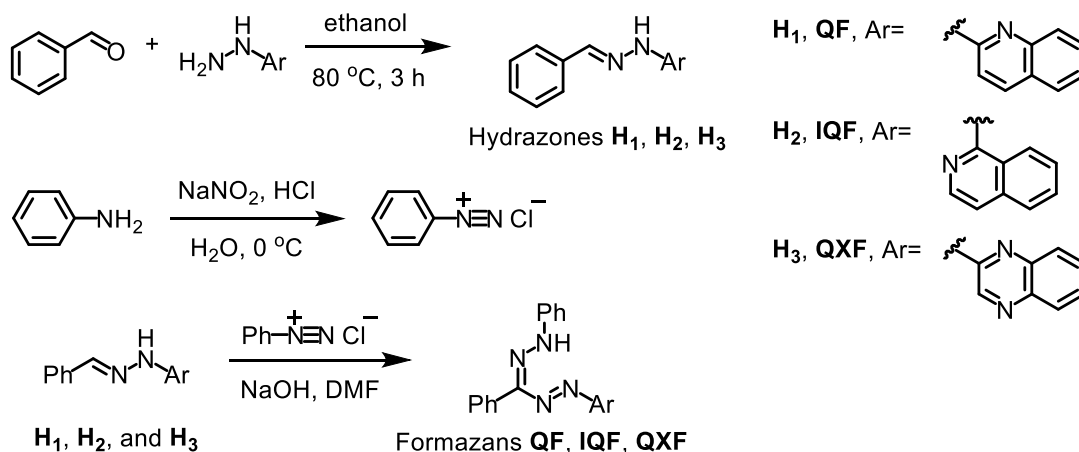
Cell-based assays in 96-well plates were conducted on a BioTek Synergy™ 2 microplate reader. Flow cytometric analyses were performed at the University of Arizona Flow Cytometry Shared Resource using a FACSCanto II flow cytometer (BDBiosciences, San Jose, CA) equipped with a 488 nm, air-cooled, 20 mW solid-state laser. Chemiluminescence signals were captured and analyzed on a Bio-Rad ChemDoc M.D. Universal Hood III Gel Documentation System.

## 2. Synthesis of formazan compounds

Precursor hydrazones  $\text{H}_1$ <sup>1</sup> and  $\text{H}_3$ <sup>2</sup> (Scheme S1) were synthesized according to published procedures. Iron chelator deferasirox (DFX) was also synthesized as previously reported.<sup>3</sup>

**Synthesis of hydrazone  $\text{H}_2$ .** A mixture of benzaldehyde (5.0 mmol) and 1-hydrazinylisoquinoline<sup>4</sup> ( $\text{ArN}_2\text{H}_3$ , 5.0 mmol) in ethanol (40 mL) was heated at reflux for 3 h (until TLC indicated that condensation was complete). The reaction mixture was cooled down in an ice bath and the precipitate was collected by filtration. The solid was washed with ice-cold ethanol and dried under vacuum. This product was used in the next step without purification.

$\text{H}_2$ , (*E*)-1-(2-benzylidenehydrazineyl)isoquinoline. Yield: 75%  $^1\text{H}$  NMR (500 MHz,  $\text{DMSO-}d_6$ )  $\delta$  10.82 (s, 1H), 8.47 (s, 1H), 8.34 (d,  $J$  = 8.2 Hz, 1H), 8.01 – 7.89 (m, 2H), 7.59 – 7.55 (m, 1H), 7.51 – 7.35 (m, 5H), 7.12 (dd,  $J$  = 7.1, 5.7 Hz, 1H), 6.31 (dd,  $J$  = 7.2, 1.3 Hz, 1H).  $^{13}\text{C}$  NMR (126 MHz,  $\text{DMSO-}d_6$ )  $\delta$  152.8, 151.7, 136.4, 136.2, 131.8, 129.7, 129.6, 129.0, 128.0, 126.8, 126.3, 125.1, 124.7, 104.2. LRMS-ESI: calcd for  $\text{C}_{16}\text{H}_{14}\text{N}_3$   $[\text{M}+\text{H}]^+$ :  $m/z$  248.12; found:  $m/z$  248.12.



**Scheme S1.** General synthetic sequence for formazan compounds.

**Synthesis of formazan compounds.** Aniline (186 mg, 2.0 mmol) was dissolved in a HCl solution (0.6 M, 20 mL) and then cooled down in an ice bath.  $\text{NaNO}_2$  (166 mg, 2.4 mmol) was dissolved in deionized water (20 mL) and added dropwise. The temperature was kept at 0 °C, and the mixture was stirred for 1 h after adding all the  $\text{NaNO}_2$  solution. The hydrazone (1.5 mmol) was dissolved in dimethylformamide (20 mL), and then aqueous NaOH (15 M, 1 mL) was added. The synthesized diazonium solution was then added slowly into the hydrazone solution at 0 °C, and the temperature was gradually warmed up to room temperature. The reaction mixture was stirred for 6 h. The precipitated crude formazan was collected by filtration. The filtrate was extracted with ethyl acetate (20 mL  $\times$  2), then the combined organic layers were washed with deionized water (10 mL  $\times$  2), dried over anhydrous  $\text{Na}_2\text{SO}_4$ , and evaporated to collect a crude solid. The precipitate from the reaction mixture and the crude solid from the extraction were combined and purified by column chromatography (hexanes/ethyl acetate, 2:1).

A minor fraction of a conformational isomer was observed in the NMR spectra of the isolated formazans in  $\text{CDCl}_3$ . As previously reported for this class of compounds,<sup>5-7</sup> the relative ratios and interconversion of the conformational isomers is affected by the identity of the substituents, solvents and exposure to light. In our case, reverse-phase HPLC analysis only showed one peak (95% or higher) for each of the isolated formazans (Fig. S1), which were employed for testing of biological activity.

**QF**, 3,5-diphenyl-1-(quinolin-2-yl)formazan. Yield: 65%, 342 mg (0.98 mmol). Minor fraction of conformational isomer observed in the NMR spectra.  $^1\text{H}$  NMR (500 MHz,  $\text{CDCl}_3$ )  $\delta$  13.89 (s, 1H), 8.18 – 8.01 (m, 6H), 7.88 – 7.82 (m, 1H), 7.76 – 7.69 (m, 1H), 7.67 – 7.64 (m, 1H), 7.60 – 7.55 (m, 3H), 7.50 – 7.47 (m, 2H), 7.44 – 7.31 (m, 2H).  $^{13}\text{C}$  NMR (126 MHz,  $\text{CDCl}_3$ )  $\delta$  155.6, 152.9, 147.4, 147.1, 142.8, 138.9, 138.6, 136.2, 132.2, 131.3, 130.3, 130.20, 130.17, 129.64, 129.57, 129.5, 129.1, 128.5, 128.0, 127.9, 127.4, 127.1, 126.7, 126.1, 124.5, 124.3, 123.2, 123.1, 110.3, 109.9. HRMS-ESI: calcd for  $\text{C}_{22}\text{H}_{18}\text{N}_5$   $[\text{M}+\text{H}]^+$ :  $m/z$  352.1557; found:  $m/z$  352.1555. Purity (HPLC, Fig. S1): 98%.

**IQF**, 1-(isoquinolin-1-yl)-3,5-diphenylformazan. Yield: 21%.  $^1\text{H}$  NMR (500 MHz,  $\text{CDCl}_3$ )  $\delta$  12.09 (s, 0.01H), 8.33 – 8.14 (m, 3H), 7.95 – 7.90 (m, 2H), 7.62 – 7.32 (m, 12H).  $^{13}\text{C}$  NMR (126 MHz,  $\text{CDCl}_3$ )  $\delta$  152.8, 144.2, 141.4, 131.7, 131.1, 129.8, 129.6, 129.2, 129.0, 128.89, 128.86, 127.4, 127.3, 127.2, 125.7, 123.0, 122.5, 120.0. HRMS-ESI: calcd for  $\text{C}_{22}\text{H}_{18}\text{N}_5$   $[\text{M}+\text{H}]^+$ :  $m/z$  352.1557; found:  $m/z$  352.1557. Purity (HPLC, Fig. S1): 98%.

**QXF**, 3,5-diphenyl-1-(quinoxalin-2-yl)formazan. Yield: 81%, 423 mg (1.2 mmol).  $^1\text{H}$  NMR (500 MHz,  $\text{CDCl}_3$ )  $\delta$  13.66 (s, 1H), 9.51 (s, 1H), 8.09 – 8.02 (m, 5H), 7.83 (d,  $J = 8.2$  Hz, 1H), 7.70 – 7.66 (m, 1H), 7.58 – 7.56 (m, 3H), 7.51 – 7.41 (m, 4H).  $^{13}\text{C}$  NMR (126 MHz,  $\text{CDCl}_3$ )  $\delta$  152.7, 150.0, 143.9, 141.0, 139.9, 136.5, 135.4, 132.8, 130.7, 129.6, 129.4, 129.0, 128.6, 127.34, 127.26, 127.1, 123.3. HRMS-ESI: calcd for  $\text{C}_{22}\text{H}_{17}\text{N}_6$   $[\text{M}+\text{H}]^+$ :  $m/z$  353.1515; found:  $m/z$  353.1509. Purity (HPLC, Fig. S1): 95%.

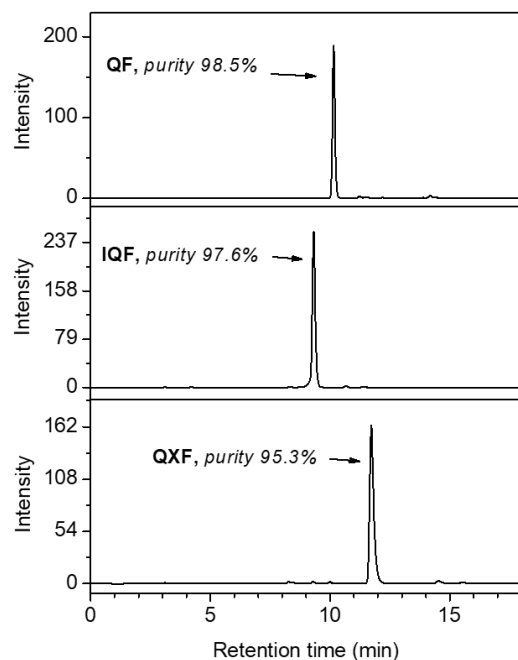


**Figure S1.** HPLC analysis of isolated formazan compounds. **QF**, **IQF**, and **QXF** were detected at 450 nm with the following method: 50:50% water/MeCN to 100% MeCN (0 → 5.0 min); 100% MeCN (5.0 → 15 min); 100% MeCN to 50:50% water/MeCN (15 → 18 min). The mobile phases contained 0.1% formic acid and the flow rate was 1 mL/min.

### 3. Iron-binding tests in buffered aqueous solutions of formazan compounds

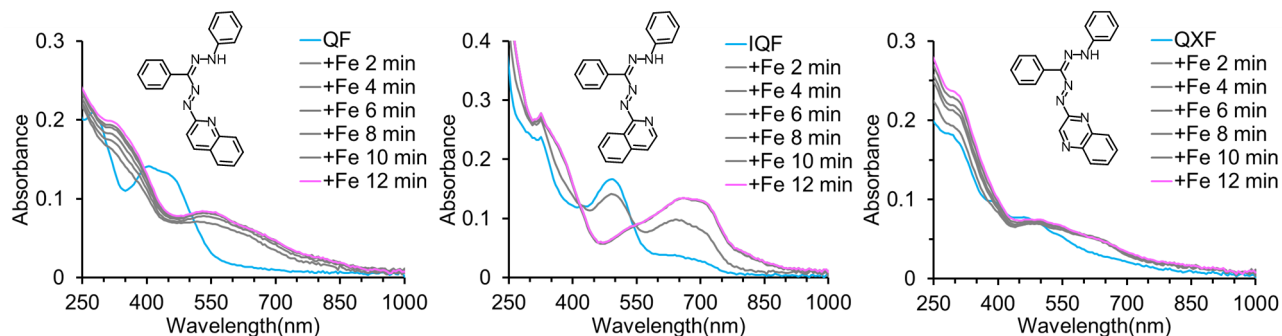
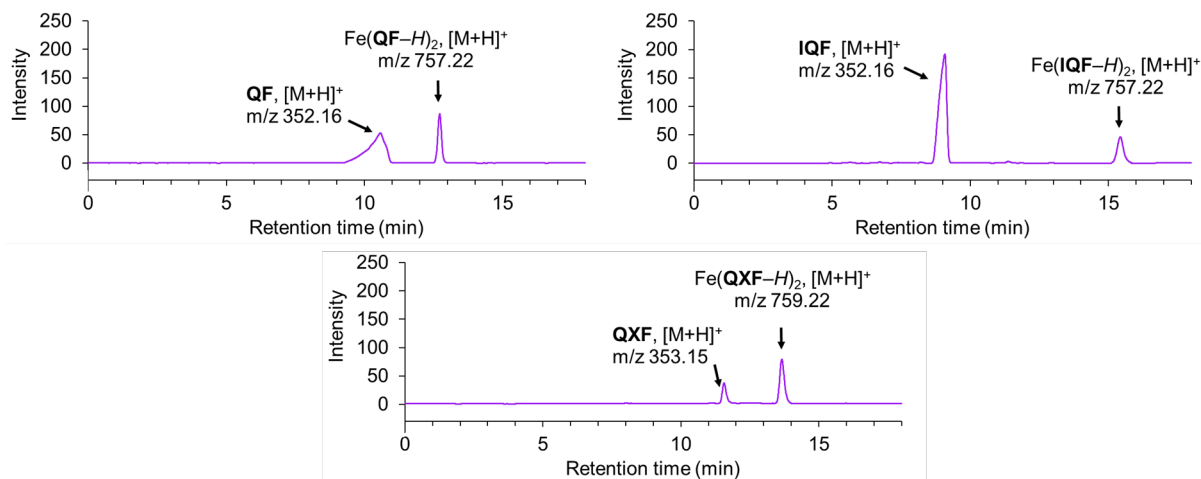


**Figure S2.** Iron binding by formazan compounds as monitored by optical absorption spectroscopy. Absorbance changes after addition of 1.0 equiv. Fe(II) (from a ferrous ammonium sulfate stock solution in degassed water) to solutions of formazan ligands (30  $\mu\text{M}$ ) in a mixture of degassed 50 mM HEPES buffer and DMSO (7:3, v/v) at pH 7.4 for 12 min.



Iron complexes	Chemical formula	Calculated $m/z$ $[M+H]^+$	Found $m/z$ $[M+H]^+$
$[\text{Fe}(\text{QF}-\text{H})_2]$	$[\text{C}_{44}\text{H}_{33}\text{FeN}_{10}]^+$	757.22	757.22
$[\text{Fe}(\text{IQF}-\text{H})_2]$	$[\text{C}_{44}\text{H}_{33}\text{FeN}_{10}]^+$	757.22	757.22
$[\text{Fe}(\text{QXF}-\text{H})_2]$	$[\text{C}_{42}\text{H}_{31}\text{FeN}_{12}]^+$	759.21	759.22

**Figure S3.** HPLC analysis of formazan solutions (200  $\mu\text{M}$ ) upon addition of ferrous ammonium sulfate (1.0 equiv.). Reactions were conducted in degassed aqueous solutions (50 mM HEPES, pH 7.4 and DMSO, 7:3, v/v) and allowed to stir for 20 min. Chromatograms were collected at 450 nm. The identity of the observed species was confirmed by LRMS-ESI.

#### 4. Synthesis and structural characterization of $\text{Fe}(\text{QF}-\text{H})_2$

**$\text{Fe}(\text{QF}-\text{H})_2$ .** The **QF** ligand (70 mg, 0.20 mmol) was dissolved in ethanol (20 mL), and  $\text{Fe}(\text{BF}_4)_2 \cdot 6\text{H}_2\text{O}$  (34 mg, 0.10 mmol) was added to the solution. The mixture was stirred for 4 h at room temperature under aerobic conditions. The precipitate was collected by filtration and washed with a mixture of water and ethanol (1:1 v/v, 10 mL). The collected solid was redissolved in dichloromethane and purified by column chromatography (hexanes/ethyl acetate, 2:1). Yield: 63%, 95 mg (0.13 mmol).  $^1\text{H}$  NMR (500 MHz,  $\text{CD}_2\text{Cl}_2$ )  $\delta$  8.58 (d,  $J = 7.8$  Hz, 4H), 7.77 (d,  $J = 8.8$  Hz, 2H), 7.63 (q,  $J = 8.1$  Hz, 6H), 7.49 (t,  $J = 7.5$  Hz, 2H), 7.35 – 7.14 (m, 8H), 7.03 (m, 6H), 6.24 (d,  $J = 8.0$  Hz, 4H).  $^{13}\text{C}$  NMR (126 MHz,  $\text{CD}_2\text{Cl}_2$ )  $\delta$  170.2, 158.0, 152.8, 147.3, 139.0, 132.5, 130.9, 129.3, 128.8, 128.6, 128.4, 128.3, 127.6, 127.5, 123.8, 123.3, 123.2, 116.8. Anal. Calcd for:  $\text{C}_{44}\text{H}_{32}\text{FeN}_{10}$ : C, 69.8; H, 4.3; N, 18.5. Found: C, 69.6; H, 4.6; N, 18.6. HRMS-ESI: calcd for  $\text{C}_{44}\text{H}_{33}\text{FeN}_{10}$   $[M+H]^+$ :  $m/z$  757.2234; found:  $m/z$  757.2329.

**X-ray diffraction analysis.** The single-crystal X-ray diffraction measurements were performed at the XRD Facility (RRID:SCR\_022886) of the University of Arizona Department of Chemistry and Biochemistry using a Bruker D8 Venture instrument equipped with Mo  $\text{I}\mu\text{S}$  3.0 microfocus source and Photon 3 detector. The diffraction data were collected at 100 K. The instrument was controlled by the *APEX5* software package (Bruker). The collected diffraction data were corrected for absorption effects using a multi-scan method in

*SADABS* (Sheldrick, G. M. University of Göttingen, Germany, 1997). The crystal structures were solved and refined with the SHELX package<sup>8</sup> from the Olex2<sup>9</sup> graphic environment. All wholly occupied non-H atoms were located in the Fourier map and refined anisotropically. Carbon-bound hydrogen atoms were calculated in ideal positions with isotropic displacement parameters set to  $1.2U_{iso}$  of the attached atom ( $1.5U_{iso}$  for methyl hydrogen atoms). Their positions were then refined using a riding model. The details of structure refinement are shown in **Table S1**, and selected bond lengths are provided in **Table S2**.\_

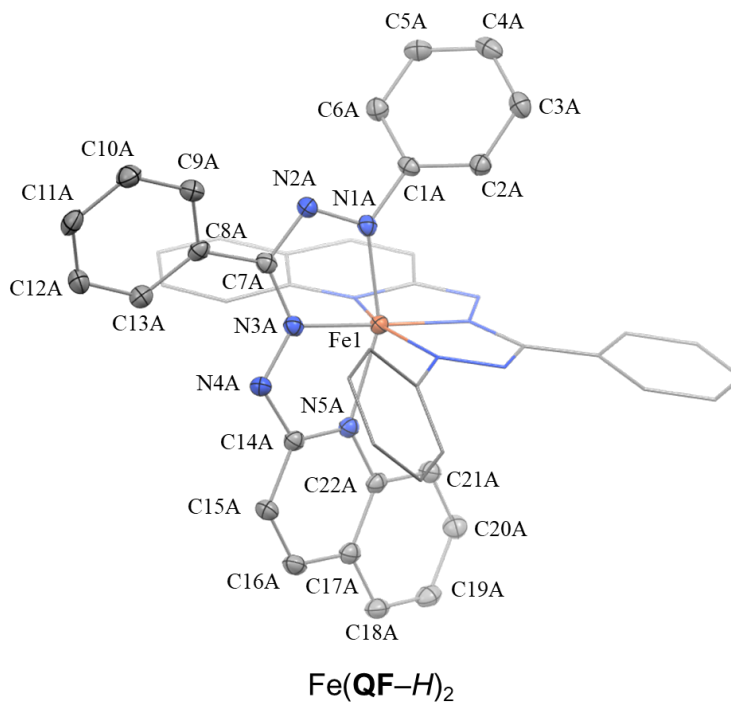
**Structure refinement of *Fe(QF-H)*<sub>2</sub>**. Crystals grew as purple plates by slow evaporation of CH<sub>2</sub>Cl<sub>2</sub>/pentane. Data were solved and refined in the triclinic, space group P-1. The unit cell contains two complexes, with one complex per asymmetric unit. The highest residual Fourier peak found in the model was 0.63 e Å<sup>-3</sup> approx. 1.04 Å from Fe1 and the deepest Fourier hole was -0.62 e Å<sup>-3</sup> approx. 0.76 Å from Fe1.

**Table S1.** Crystallographic information for **Fe(QF-H)<sub>2</sub>**.

<b>Complex</b>	<b>Fe(QF-H)<sub>2</sub></b>
Empirical formula	C <sub>44</sub> H <sub>32</sub> FeN <sub>10</sub>
Formula weight/g•mol <sup>-1</sup>	756.64
Temperature/K	100.0
Crystal system	triclinic
Space group	P-1
a/Å	9.8316(11)
b/Å	10.5680(10)
c/Å	17.2201(18)
α/°	81.653(3)
β/°	83.058(4)
γ/°	85.688(3)
Volume/Å <sup>3</sup>	1754.2(3)
Z	2
ρ <sub>calc</sub> /cm <sup>3</sup>	1.432
μ/mm <sup>-1</sup>	0.480
F(000)	784.0
Crystal size/mm <sup>3</sup>	0.15 × 0.093 × 0.03
Radiation	MoKα (λ = 0.71073)
2θ range for data collection/°	4.18 to 52.838
Index ranges	-12 ≤ h ≤ 12, -11 ≤ k ≤ 13, -21 ≤ l ≤ 21
Reflections collected	42979
Independent reflections	7161 [R <sub>int</sub> = 0.0978, R <sub>sigma</sub> = 0.0606]
Data/restraints/parameters	7161/0/496
Goodness-of-fit on F <sup>2</sup>	1.045
Final R indexes [I ≥ 2σ (I)]	R <sub>1</sub> = 0.0467, wR <sub>2</sub> = 0.1050
Final R indexes [all data]	R <sub>1</sub> = 0.0658, wR <sub>2</sub> = 0.1168
Largest diff. peak/hole / e Å <sup>-3</sup>	0.63/-0.62
CCDC	2336932

<sup>a</sup> R<sub>1</sub> =  $\sum [|F_o| - |F_c|] / \sum |F_o|$ ; <sup>b</sup> wR<sub>2</sub> =  $[\sum w(F_o^2 - F_c^2) / \sum wF_o^4]^{1/2}$

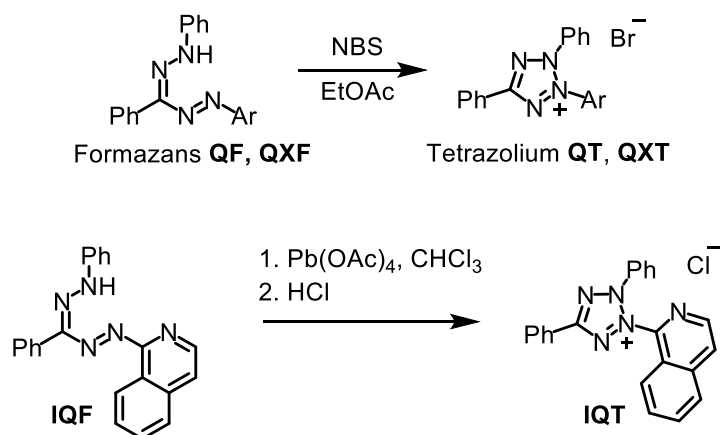
**Table S2.** Selected bond lengths (Å) for the crystal structure of **Fe(QF-H)<sub>2</sub>**.



Bonds (ligand A & B)	Length (Å)	Bonds (ligand A & B)	Length (Å)
N1–Fe1	1.935(2)	N3–C7	1.355(3)
	1.923(2)		1.350(3)
N3–Fe1	1.862(2)	N1–C1	1.424(3)
	1.872(2)		1.427(3)
N5–Fe1	2.038(2)	C7–C8	1.471(3)
	2.031(2)		1.474(3)
N1–N2	1.309(3)	N4–C14	1.365(3)
	1.305(3)		1.363(3)
N3–N4	1.335(3)	N5–C14	1.351(3)
	1.342(3)		1.347(3)
N2–C7	1.347(3)		
	1.355(3)		



## 5. Synthesis of tetrazolium compounds



**Scheme S2.** General scheme for the synthesis of tetrazolium compounds **QT**, **QXT**, and **IQT**.

**Synthesis of QT and QXT.** A solution of *N*-bromosuccinimide (NBS, 160 mg, 0.9 mmol) in ethyl acetate (20 mL) was added to a solution of formazan (0.6 mmol: 211 mg **QF** or **QXF**) in ethyl acetate (20 mL). The reaction was stirred at room temperature for 12 h, and then cooled in a refrigerator (4 °C) for 1 h. The desired products were isolated by filtration, dried under vacuum, and collected as light-yellow solids.

**QT**, 2,5-diphenyl-3-(quinolin-2-yl)-tetrazolium bromide. Yield: 78%, 201 mg (0.47 mmol). <sup>1</sup>H NMR (500 MHz, DMSO-*d*<sub>6</sub>) δ 9.01 (d, *J* = 8.9 Hz, 1H), 8.39 (t, *J* = 7.7 Hz, 3H), 8.28 (d, *J* = 8.2 Hz, 1H), 8.03 – 7.94 (m, 3H), 7.92 – 7.75 (m, 7H), 7.61 (d, *J* = 8.1 Hz, 1H). <sup>13</sup>C NMR (126 MHz, DMSO-*d*<sub>6</sub>) δ 163.9, 145.0, 144.5, 142.4, 135.6, 133.71, 133.70, 132.8, 130.5, 130.2, 130.0, 129.0, 128.7, 128.5, 127.4, 126.2, 122.8, 116.2. HRMS-ESI: calcd for C<sub>22</sub>H<sub>16</sub>N<sub>5</sub> [M]<sup>+</sup>: *m/z* 350.1401; found: *m/z* 350.1400. Purity (HPLC, Fig. S4): 96%.

**QXT**, 2,5-diphenyl-3-(quinoxalin-2-yl)-tetrazolium bromide. Yield: 45%, 194 mg (0.24 mmol). <sup>1</sup>H NMR (400 MHz, DMSO-*d*<sub>6</sub>) δ 9.79 (s, 1H), 8.46 – 8.36 (m, 3H), 8.22 – 8.16 (m, 1H), 8.11 – 8.02 (m, 3H), 7.94 – 7.75 (m, 7H). <sup>13</sup>C NMR (101 MHz, DMSO-*d*<sub>6</sub>) δ 164.3, 143.0, 140.7, 140.0, 137.8, 135.0, 134.6, 134.1, 133.9, 133.6, 130.2, 130.1, 129.4, 129.0, 127.6, 126.4, 122.6. HRMS-ESI: calcd for C<sub>21</sub>H<sub>15</sub>N<sub>6</sub> [M]<sup>+</sup>: *m/z* 351.1353; found: *m/z* 351.1352. Purity (HPLC, Fig. S4): 97%.

**Synthesis of IQT.** Lead tetraacetate (PbOAc<sub>4</sub>) was recrystallized from glacial acetic acid and collected as a white crystalline solid. A solution of lead tetraacetate (151 mg, 0.34 mmol) in chloroform (3 mL) was added to a solution of formazan (0.28 mmol: 100 mg **IQF**) in chloroform (3 mL). The reaction was stirred at 4 °C for 4 h as the color of the mixture changed from red pink to brown. The reaction mixture was concentrated and then HCl (2 M, 10 mL) was added. The mixture was poured into dichloromethane (10 mL) and transferred to a separatory funnel. The aqueous layer was washed two more times with dichloromethane (10 mL), then the combined organic layers were dried over anhydrous Na<sub>2</sub>SO<sub>4</sub>. Following evaporation, the crude product was purified by gradient column chromatography (0–15% CH<sub>3</sub>OH in CH<sub>2</sub>Cl<sub>2</sub>).

**IQT**, 3-(isoquinolin-1-yl)-2,5-diphenyl-tetrazolium chloride. Yield: 32%, 34.6 mg (0.09 mmol). <sup>1</sup>H NMR (500 MHz, CD<sub>3</sub>OD) δ 8.49 – 8.43 (m, 3H), 8.36 – 8.27 (m, 3H), 8.12 – 7.96 (m, 2H), 7.89 – 7.74 (m, 6H), 7.66 – 7.60 (m, 2H). <sup>13</sup>C NMR (126 MHz, CD<sub>3</sub>OD) δ 167.4, 145.0, 142.1, 140.7, 135.7, 135.3, 134.9, 134.3,

132.8, 131.5, 131.1, 129.1, 129.0, 128.9, 126.6, 124.5, 123.8, 123.7. HRMS-ESI: calcd for  $C_{22}H_{16}N_5 [M]^+$ :  $m/z$  350.1401; found:  $m/z$  350.1400. Purity (HPLC, Fig. S4): 98%.

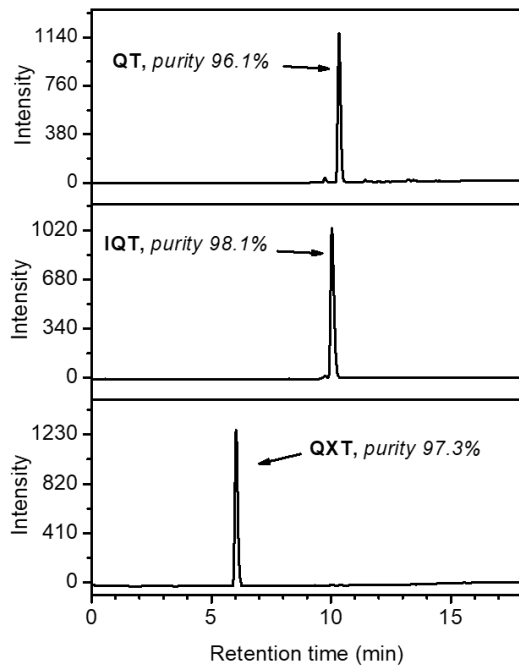


**Figure S4.** HPLC analysis of purified tetrazolium compounds. **QT**, **IQT**, and **QXT** were detected at 254 nm with the following method: 100% water to 100% MeOH (0 → 12 min); 100% MeOH (12 → 15 min); 100% MeOH to 100% water (15 → 18 min). The mobile phases contained 0.1% formic acid and the flow rate was 1 mL/min.

## 6. Solution properties of tetrazolium compounds

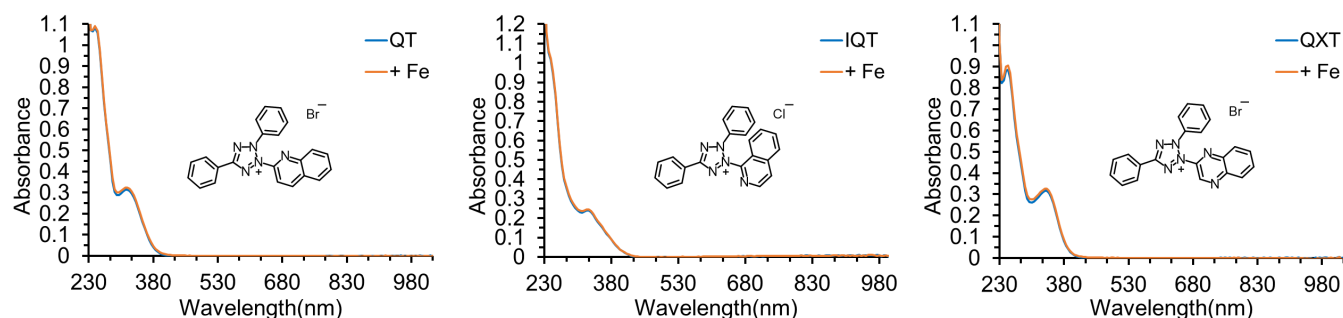


**Figure S5.** Optical absorption spectra before and after addition of 1 equiv. Fe(II) (from a ferrous ammonium sulfate stock solution in degassed water) to solutions of tetrazolium salts (30  $\mu\text{M}$ ) in a degassed mixture of HEPES buffer (50 mM, pH 7.4) and DMSO (7:3, v/v) over a period of 10 min.

**Octanol/PBS distribution coefficients ( $\log D_{\text{o/pH}7.4}$ , Table S3).** The shake-flask method was used to determine the  $\log D_{\text{o/pH}7.4}$  values of the tetrazolium compounds (QT, IQT, and QXT).<sup>10</sup> The tetrazolium salts were dissolved in PBS (pH 7.4, 2 mL) to reach a final concentration of 1 mM. Each PBS solution containing the tetrazolium compound (1 mL) was mixed with octanol (1 mL) that was pre-saturated with PBS (pH 7.4). The two phases were shaken vigorously at room temperature for 12 h and then separated by centrifugation. The concentration of tetrazolium in the two phases was determined by HPLC. The  $\log D_{\text{o/pH}7.4}$  values were calculated from an average of three independent measurements.

Given the extended  $\pi$  system of the coordinating heterocycles, the obtained values for QT and IQT were around 1.0, significantly higher than that reported for *N*-pyridyl tetrazolium **2b** ( $\log D_{\text{o/pH}7.4} = -0.5$ ).<sup>10</sup> The additional nitrogen rendered the quinoxaline system QXT more hydrophilic than the quinoline ones, with a  $\log D_{\text{o/pH}7.4}$  of 0.4.

*Note:* The concentrations of formazan compounds in the PBS phase were below HPLC detection limit; therefore, the  $\log D_{\text{o/pH}7.4}$  values could not be determined by this method.

**Table S3.** Distribution coefficients  $\log D_{\text{o/pH}7.4}$  values determined by HPLC using the shake-flask method in octanol and PBS (pH 7.4).

Compound	$\log D_{\text{o/pH}7.4}$
DFX	1.3
QT	1.0
IQT	0.9
QXT	0.4

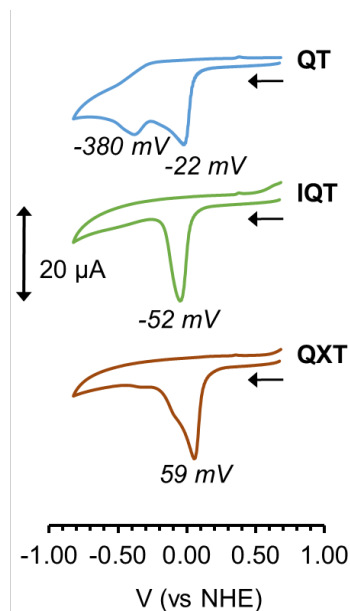


**Figure S6.** Cyclic voltammograms ( $100 \text{ mV s}^{-1}$ ) of tetrazolium compounds (2 mM in PBS, pH 7.4) recorded at a 2.0 mm-diameter glassy carbon working electrode, using a platinum auxiliary electrode and an Ag/AgCl reference electrode in 1 M KCl. Potassium ferricyanide ( $\text{K}_3[\text{Fe}(\text{CN})_6]$ ) was used as a reference ( $E_0 = 0.430 \text{ V vs. NHE}$ , aqueous  $25 \text{ }^\circ\text{C}$ ).<sup>11</sup>

**Reduction of tetrazolium compounds by ascorbate or glutathione.** The tetrazolium salts (100  $\mu\text{M}$ ) were stirred in the presence of sodium ascorbate or glutathione (5 mM) at pH 7.4 (100 mM phosphate buffer/DMSO, 7:3 v/v) at  $37 \text{ }^\circ\text{C}$ . At each time point (0, 1, 2, 3, 4, 5, 6, 7, 8, 9, and 24 h), a 40  $\mu\text{L}$  aliquot was injected for HPLC analysis, and the reaction progress was monitored at 254 nm.

**Stability of tetrazolium compounds in fetal bovine serum (FBS).** Each compound was added to neat FBS (Corning 35-010-CV, USDA Approved Origin) to a 1.0 mM final concentration (0.5% DMSO in 1.0 mL FBS). The samples were protected from light and incubated at  $37 \text{ }^\circ\text{C}$ . At each time point (0, 2, 4, 6, 8, 10, 12, 24, 48, and 72 h), an aliquot (100  $\mu\text{L}$ ) was transferred out for testing. Before injection, the aliquot was added to  $\text{CH}_3\text{OH}$  (400  $\mu\text{L}$ ) to precipitate most protein components. The precipitates were removed by centrifugation (14,000 rpm for 5 min) and the supernatant was analyzed by HPLC. The chromatograms were detected at 254 nm. The degradation of tetrazolium salts was determined based on the change of peak area relative to the initial value (at 0 h).

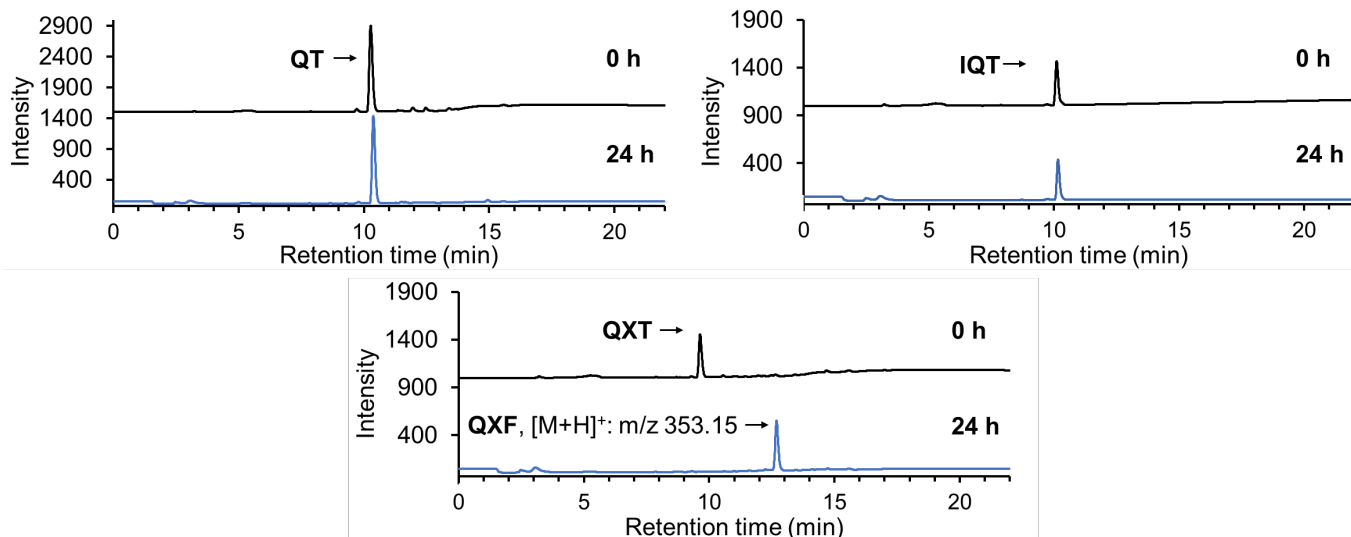


**Figure S7.** HPLC analysis of the stability of tetrazolium compounds in fetal bovine serum (FBS). The chromatograms at 0 h and 24 h were detected at 254 nm. The identity of the degradation products (if any) was confirmed by LC-MS.

### 7. Cell-based assays and biological characterization

The A2780 (Fox Chase Cancer Center, 03-26) cells were grown in RPMI-1640 medium (Corning) supplemented with 10% FBS, penicillin (100 I.U./mL) and streptomycin (100  $\mu\text{g}/\text{mL}$ , Cytiva HyClone). MDA-MB-231 (ATCC<sup>®</sup> HTB-26<sup>™</sup>), MRC-5 (ATCC<sup>®</sup> CCL-171<sup>™</sup>) cell lines were maintained in Eagle's Minimum Essential Medium (EMEM, Corning) supplemented with 10% FBS, penicillin and streptomycin. All cells were cultured at 37 °C in a humidified atmosphere containing 5% CO<sub>2</sub>.

**Cell viability assays.** Cell viability was assessed by standard methods using the resazurin dye. Cells were seeded in full growth media (100  $\mu\text{L}$ ) with the following cell density per well in black 96-well plates: A2780, 3000 cells/well; MDA-MB-231, 4000 cells/well; MRC-5, 5000 cells/well, and allowed to attach for at least 24 h. Test compounds dissolved in DMSO were diluted in growth media to concentrations ranging from 0.032–100  $\mu\text{M}$  or 0.8–500  $\mu\text{M}$  (with final DMSO amount limited to 0.5%). Cells were incubated in the presence of the test compounds (200  $\mu\text{L}$  in growth media) for 72 h. A resazurin stock solution (5 mg of the dye was dissolved in 25 mL of DPBS) was added to each well (20  $\mu\text{L}$ ) and incubated at 37 °C until the color of untreated wells changed from blue to pink (2 to 3 h). Fluorescence emission was recorded on a BioTek Synergy<sup>™</sup> 2 microplate reader (excitation: 540/35 nm, emission: 600/40 nm). The data were analyzed using logarithmic fits to obtain IC<sub>50</sub> values, which are given as mean plus/minus standard deviation for at least three independent experiments.

**Statistical Analysis.** A two-tailed t-test with two-sample equal variance was performed on Microsoft Excel. Data with *p* values lower than 0.05 were regarded as statistically significant.

**Cell cycle analysis.** Flow cytometric analyses were performed at the University of Arizona Flow Cytometry Shared Resource (Research, Innovation, and Impact / University of Arizona Cancer Center) using a FACSCanto II flow cytometer (BDBiosciences, San Jose, CA) equipped with a 488 nm, air-cooled, 20 mW solid-state laser. The fluorescence of propidium iodide (PI) was measured and recorded through a 585nm/42nm bandpass filter into a photomultiplier detector. List mode data files consisting of 10,000 events were gated on single cells by using a doublet discrimination method of plotting PI fluorescence area versus PI peak channel intensity (PI-A vs. PI-H) in Diva 8.0 (BD Biosciences, San Jose, CA). Quantification of the phases of the cell cycle ( $G_0/G_1$ , S, and  $G_2/M$ ) was performed using ModFit LT (Verity Software House, Topsham, ME).

A2780 cells were seeded at  $2 \times 10^5$  cells per well in 6-well plates and allowed to adhere for 48 h at 37 °C. The media were then replaced with fresh media containing the test compounds (DFX 50  $\mu$ M, QT and IQT 5  $\mu$ M, 0.2% DMSO), and the cultures were incubated for 24 h. Cells were washed with DPBS (1 mL  $\times$  2) and then detached by addition of 0.25% trypsin-EDTA (0.4 mL) followed by a 2-min incubation. After the addition of growth media (1 mL), the cell suspension was centrifuged at 1100 rpm for 5 min. Media were discarded and cells were fixed by addition of ice-cold 70% ethanol (2 mL) and stored in a freezer at -20 °C overnight (no longer than one week). Cells were spun at 2300 rpm for 10 min, and the resulting pellet was suspended in DPBS (0.3 mL) and then treated with DNase-free RNase A and PI (0.5 mg/mL and 40  $\mu$ g/mL respectively, 30 min), placed on ice, and analyzed by flow cytometry within 1 h.

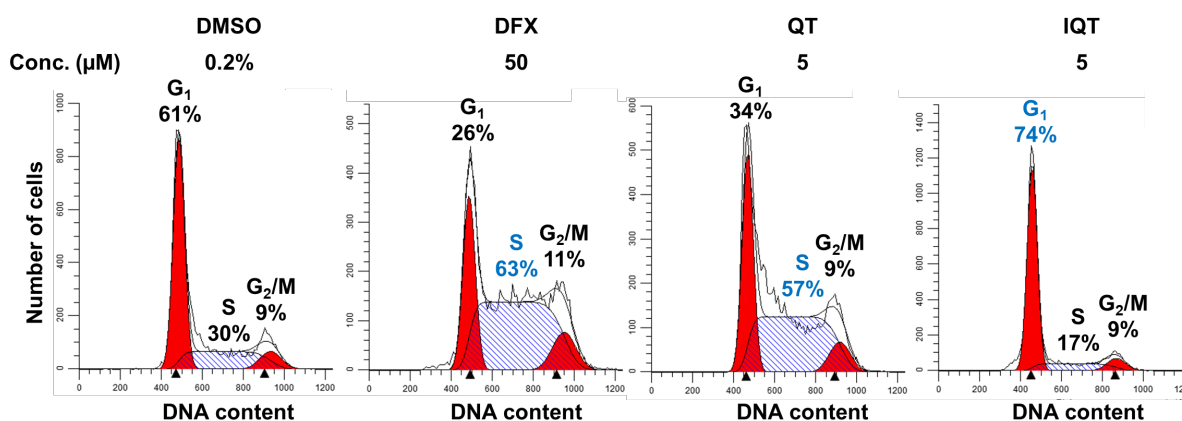


**Figure S8.** Representative cell cycle assay results in A2780 cells after treatment with the test compounds for 24 h.

**Apoptosis analysis.** A2780 cells were seeded at a density of  $3 \times 10^5$  cells per well in 6-well plates and cultured for 24 h at 37 °C. The culture media were replaced with fresh media containing the test compounds (DFX 50  $\mu$ M, QT and IQT 5  $\mu$ M, 0.2% DMSO) and incubated for 48 h. Cells were then harvested (including detached and attached cells) and washed once with cold DPBS and Annexin-binding buffer (10 mM HEPES, 140 mM NaCl, 2.5 mM  $CaCl_2$ , pH 7.4). After resuspending the pellets in Annexin-binding buffer, the cell number was determined, and the cell density was adjusted to  $1 \times 10^6$  cells/mL. Annexin V-FITC conjugate (according to the manufacturer protocol: 5  $\mu$ L for up to  $1 \times 10^6$  cells, cat# 640906, BioLegend) and propidium iodide (PI) solutions (final concentration 1  $\mu$ g/mL) were added to the cell suspensions ( $1 \times 10^5$  cells in 100  $\mu$ L binding buffer). The cells were incubated at room temperature for 15 min in the dark, then Annexin-binding buffer (400  $\mu$ L) was added and mixed gently. The prepared samples were kept on ice and analyzed by flow cytometry within 1 hour. Excitation at 488 nm and emission at 530/30 nm and 585nm/42 nm were

employed for FITC and PI, respectively. Appropriate electronic compensation was adjusted by acquiring cell populations stained with Annexin V-FITC/PI individually. For analysis, the cells were grouped in four quadrants as follows: normal (Q1, Annexin V-FITC/PI -/-), early apoptosis (Q2, Annexin V-FITC/PI +/-), late apoptosis (Q3, Annexin V-FITC/PI ++), and necrosis (Q4, Annexin V-FITC/PI -/+).

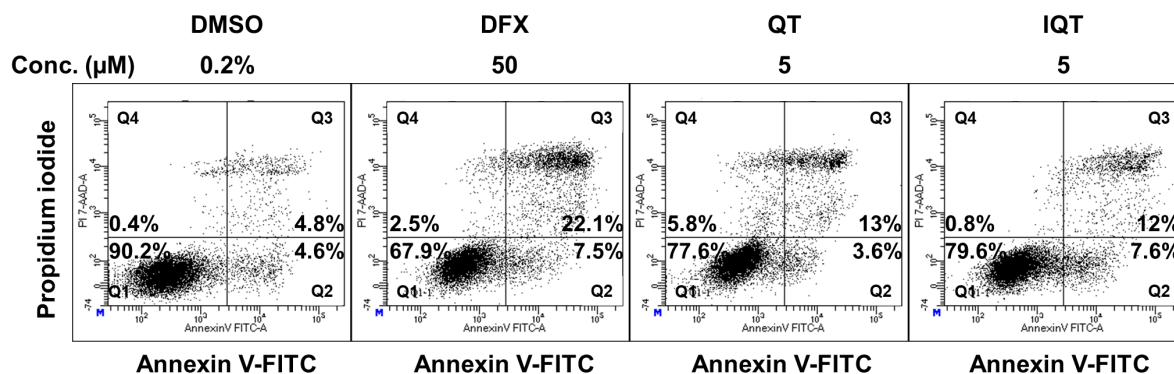


**Figure S9.** Representative apoptosis assay results in A2780 cells after treatment with the test compounds for 48 h.

**Intracellular iron binding (calcein assay).** A2780 cells were seeded at a density of  $1 \times 10^4$  cells per well in black 96-well plates and cultured for 24 h at 37 °C. The cells were washed gently with DPBS twice to remove residual FBS, and incubated with calcein-AM (0.1 μM, cat# sc-203865, Santa Cruz Biotechnology) prepared in serum-free RPMI-1640 medium (without phenol red, Quality Biological Inc cat#: 112-040-101) for 15 min at 37 °C. The cells were then washed with DPBS to remove residual calcein-AM and fresh medium was added to each well. After obtaining baseline readings of calcein fluorescence for each well, the test compounds were added in RPMI medium (5 μM, 0.2% DMSO, serum-free and without phenol red) and the plate was read after 1 h and 3 h. Fluorescence emission was recorded on a BioTek Synergy™ 2 microplate reader (excitation: 485/20 nm, emission: 528/20 nm). The calculation of fluorescence change (%) was conducted by comparing readings before and after the loading of test compounds. Data are reported as averages from three different experiments plus/minus one standard deviation.

**Detection of intracellular iron formazan complexes by uHPLC-HRMS.** A2780 cells ( $6 \times 10^6$  cells) were treated with the test compounds (5  $\mu$ M) and incubated for 48 h. The cell suspension (11 mL) was then centrifuged (1000 rpm, 8 min), and the cells were washed with cold PBS twice (1 mL), transferred to Eppendorf centrifuge tube (1.5 mL), and spun down (1000 rpm, 8 min). The cells were resuspended in cold DPBS (200  $\mu$ L) and lysed by the thermal lysis method: a freeze-thaw cycle at  $-80^\circ\text{C}$  (in a 2-propanol/dry ice bath) and room temperature (in a water bath) was repeated 5 times. The proteins and salts were then precipitated by adding cold acetone ( $-20^\circ\text{C}$ , 800  $\mu$ L) to the tubes, which were sonicated in ice cold water for 2 min and gently vortexed. The lysate mixtures were stored at  $-20^\circ\text{C}$  overnight. Next day, the tubes were centrifuged (14000 rpm, 5 min) and the supernatant (acetone and water mixture) was collected for analysis. After concentrating each sample to a volume of  $\sim 70$   $\mu$ L, the solutions were analyzed by LCMS. Briefly, LCMS analyses were performed on a Vanquish uHPLC System coupled with Q Exactive Plus mass spectrometer (Thermo Fisher Scientific, Germany). High Resolution MS analysis was performed in Full MS mode using heated electrospray ionization (HESI). MS data were collected at a resolution of 140,000 using an automatic gain control (AGC) target of  $3 \times 10^6$  with transient time of 200 ms. Spectra were collected over a mass range of  $m/z$  310 to 800 amu.

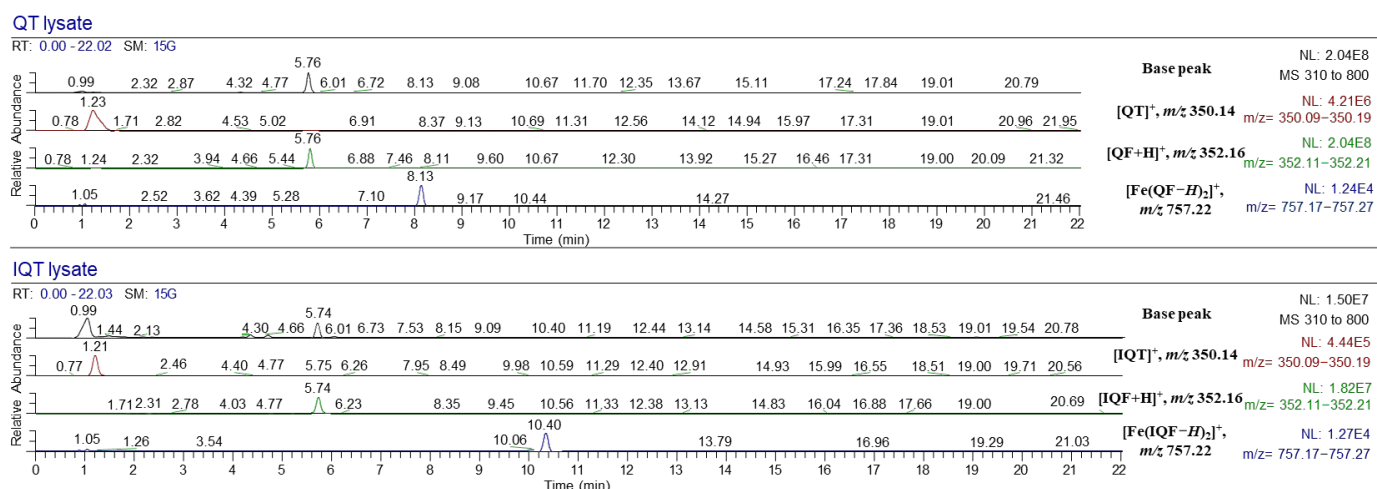


**Figure S10.** uHPLC-HRMS analysis of A2780 cell lysates after incubation with tetrazolium prochelators QT (top panel) and IQT (bottom panel). The formazan chelator and the corresponding iron complex are detected in both cases. Data are presented as base peak mass chromatograms and extracted-ion chromatograms (EIC) with the range of  $\pm 0.05$  amu of the  $m/z$  of interest (i.e., tetrazolium, formazan and 2:1 ligand-to-metal complex) and selected  $m/z$  range from 310 to 800 amu.



**Western blot analysis.** For analysis of TfR1, ferritin H, and  $\beta$ -actin expression levels, A2780 cells ( $3.5 \times 10^5$  cells/well) were seeded in 6-well plates and cultured for 24 h, then the test compounds (FAC and DFX: 50  $\mu$ M; QT and IQT: 5  $\mu$ M; 0.2% DMSO in full growth media) were added and incubated for an additional 24 h. The cells were then washed with cold DPBS, suspended in RIPA lysis buffer supplemented with protease and phosphatase inhibitor cocktail (Sigma-Aldrich PPC1010-1ML), and incubated on ice for 5 min. An aliquot was taken to determine the protein concentration by using a bicinchoninic acid-based protein assay (Thermo Fisher Scientific). 2x Laemmli sample buffer (Bio-Rad 1610737) supplemented with 5%  $\beta$ -mercaptoethanol was added in 1:1 ratio to the cell lysates prepared in RIPA buffer, and incubated at 90 °C for 5 min. The extracts were then sonicated (10% amplitude, 30 s) on ice. Whole-cell lysates (30  $\mu$ g) were loaded onto SDS-polyacrylamide gels (12.5% acrylamide for resolving TfR1 and ferritin H) and separated by electrophoresis (200 V, 45 min). A pre-stained protein ladder (10–250 kDa, Prometheus Protein Biology Products 83-660) was used as a comparison. Proteins were transferred to polyvinylidene difluoride membranes (PVDF, Bio-Rad cat# 1620174, 100 V, 1 h,) and blocked for 1 h at 22 °C in 5% (w/v) nonfat dry milk in Tris-buffered saline solution containing 0.1% (v/v) Tween-20 (TBST). After washing with TBST 3 times, the membranes were incubated overnight at 4 °C with the following primary antibodies: mouse mAb anti-CD71/TfR1 IgG<sub>1</sub> $\kappa$  (1:1000, sc-32272, Santa Cruz Biotechnology) in 1% nonfat dry milk in TBST, mouse mAb anti-ferritin heavy chain IgG<sub>2a</sub> $\kappa$  (1:1000, sc-376594, Santa Cruz Biotechnology) in 5% BSA in TBST, and mouse monoclonal anti- $\beta$ -actin (1:5000, A1978, Sigma-Aldrich) in 5% milk in TBST. On the following day, after washing with TBST 3 times, the membranes were incubated with m-IgG $\kappa$  HRP-labeled secondary antibody (1:5000, sc-516102, Santa Cruz Biotechnology) in TBST for 1 h at 22 °C. After incubation with the secondary antibody, the membranes were washed with TBST 3 times and incubated with Clarity Max Western ECL Substrate (Bio-Rad cat# 1705062). Images were captured and analyzed with a Bio-Rad ChemiDoc M.D. Universal Hood III Gel Documentation System.

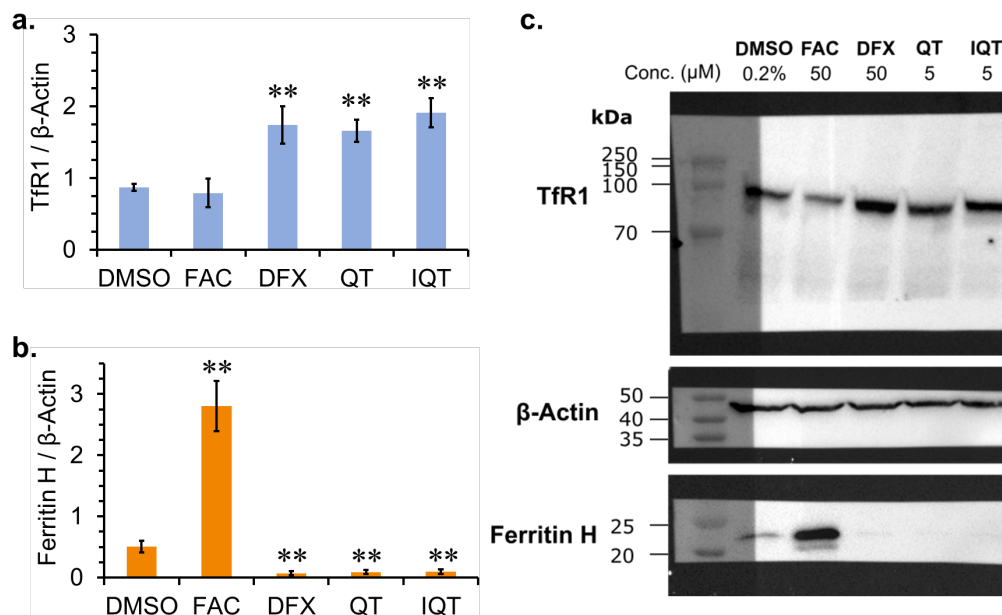
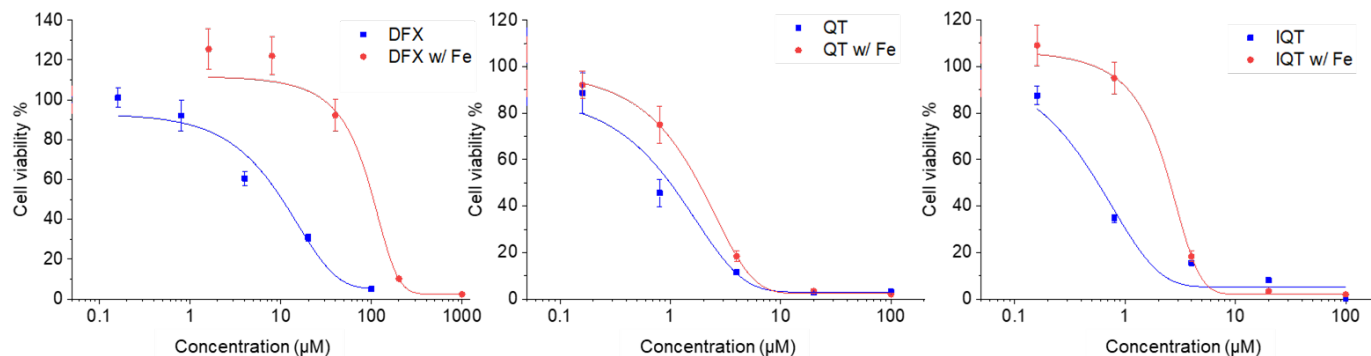


**Figure S11.** Western blot analysis of the effects of test compounds on the expression of transferrin receptor 1 (TfR1) (a) and ferritin heavy chain (ferritin H) (b) in A2780 cancer cells.  $\beta$ -Actin was used as a loading control. All *t*-tests ( $n = 3$ ) relative to vehicle only (DMSO): \*\* $p < 0.01$ . (c) Unprocessed, merged images of the raw Western blots (chemiluminescence mode) and pre-stained protein ladders (colorimetry mode) on PVDF membranes.

**Cell rescue test via iron supplementation.** The resazurin assay (*vide supra*) was employed to determine the effects of iron supplementation on the antiproliferative activities of the test compounds. In brief, A2780 cells were seeded at 3000 cells/well and allowed to attach for 24 h. A serial dilution of each compound was prepared in RPMI-1640 growth media supplemented with ferric ammonium citrate (FAC, 50  $\mu\text{M}$ ). The dose range was 1.6  $\mu\text{M}$  to 1 mM for DFX and 0.16  $\mu\text{M}$  to 100  $\mu\text{M}$  for QT and IQT. The test compounds were incubated in A2780 cell cultures for 72 hours.



Compound	IC <sub>50</sub> ( $\mu\text{M}$ , 72 h) (w/o Fe)	IC <sub>50</sub> ( $\mu\text{M}$ , 72 h) (w/ Fe)
DFX	12 $\pm$ 2	132 $\pm$ 40
QT	0.8 $\pm$ 0.1	2.6 $\pm$ 0.4
IQT	0.5 $\pm$ 0.1	3.2 $\pm$ 0.7

**Figure S12.** Representative cell viability data for the rescue tests in A2780 cells after 72-h incubations with the test compounds in the absence or presence of ferric ammonium citrate (50  $\mu\text{M}$ ) as the iron supplement.

## 8. References

1. M. Hebenbrock and J. Müller, *Z. Naturforsch. B*, 2018, **73**, 885-893.
2. F. A. R. Rodrigues, I. d. S. Bomfim, B. C. Cavalcanti, C. d. Ó. Pessoa, J. L. Wardell, S. M. S. V. Wardell, A. C. Pinheiro, C. R. Kaiser, T. C. M. Nogueira, J. N. Low, L. R. Gomes and M. V. N. de Souza, *Bioorg. Med. Chem. Lett.*, 2014, **24**, 934-939.
3. A. Steinbrueck, A. C. Sedgwick, H.-H. Han, M. Y. Zhao, S. Sen, D.-Y. Huang, Y. Zang, J. Li, X.-P. He and J. L. Sessler, *Chem. Commun.*, 2021, **57**, 5678-5681.
4. Y. Xu, B. Shen, L. Liu and C. Qiao, *Tetrahedron Lett.*, 2020, **61**, 151844.
5. A. W. Nineham, *Chem. Rev.*, 1955, **55**, 355-483.
6. A. T. Hutton and H. M. N. H. Irving, *J. Chem. Soc. Chem. Commun.*, 1980, DOI: 10.1039/C39800000763, 763-765.
7. J. B. Gilroy, P. O. Otieno, M. J. Ferguson, R. McDonald and R. G. Hicks, *Inorg. Chem.*, 2008, **47**, 1279-1286.
8. G. Sheldrick, *Acta Cryst.*, 2015, **A71**, 3-8.
9. O. V. Dolomanov, L. J. Bourhis, R. J. Gildea, J. A. K. Howard and H. Puschmann, *J. Appl. Cryst.*, 2009, **42**, 339-341.
10. Z. Xu, Y.-S. Sung and E. Tomat, *J. Am. Chem. Soc.*, 2023, **145**, 15197-15206.
11. P. Leslie Dutton, in *Methods in Enzymology*, Academic Press, 1978, vol. 54, pp. 411-435.

## 9. NMR Spectra ( $^1\text{H}$ and $^{13}\text{C}$ )

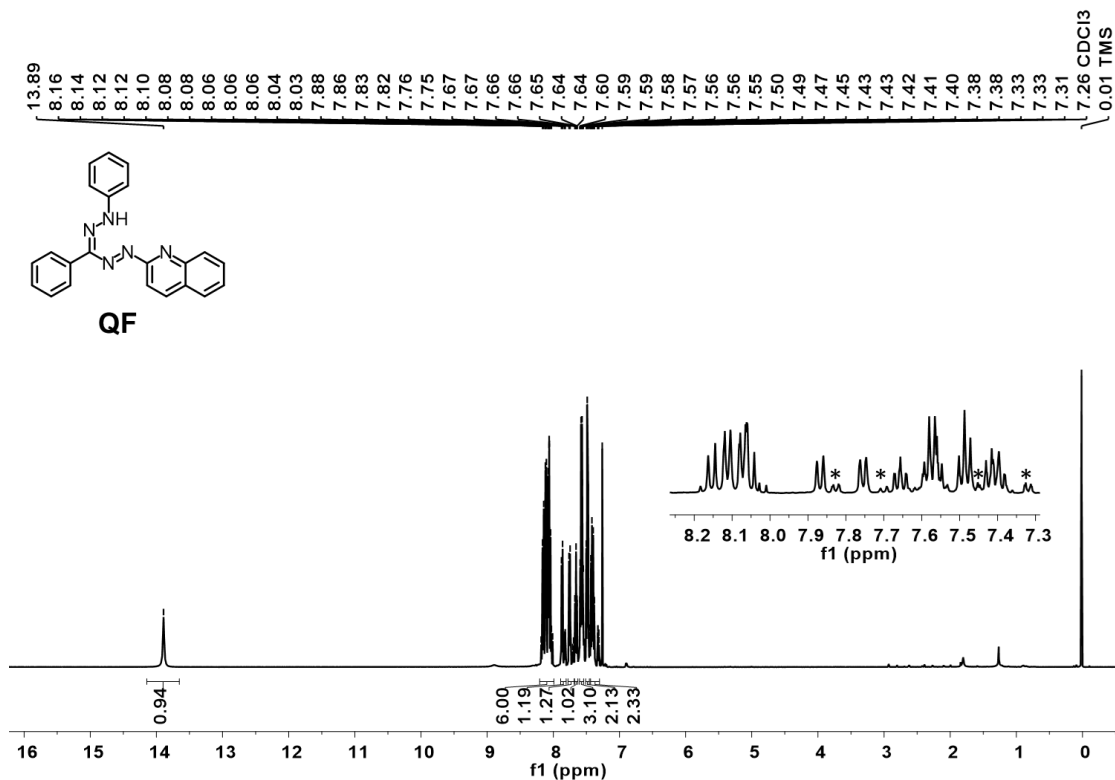


Figure S13.  $^1\text{H}$  NMR spectrum of QF (500 MHz,  $\text{CDCl}_3$ ). \*Minor fraction of conformational isomer.

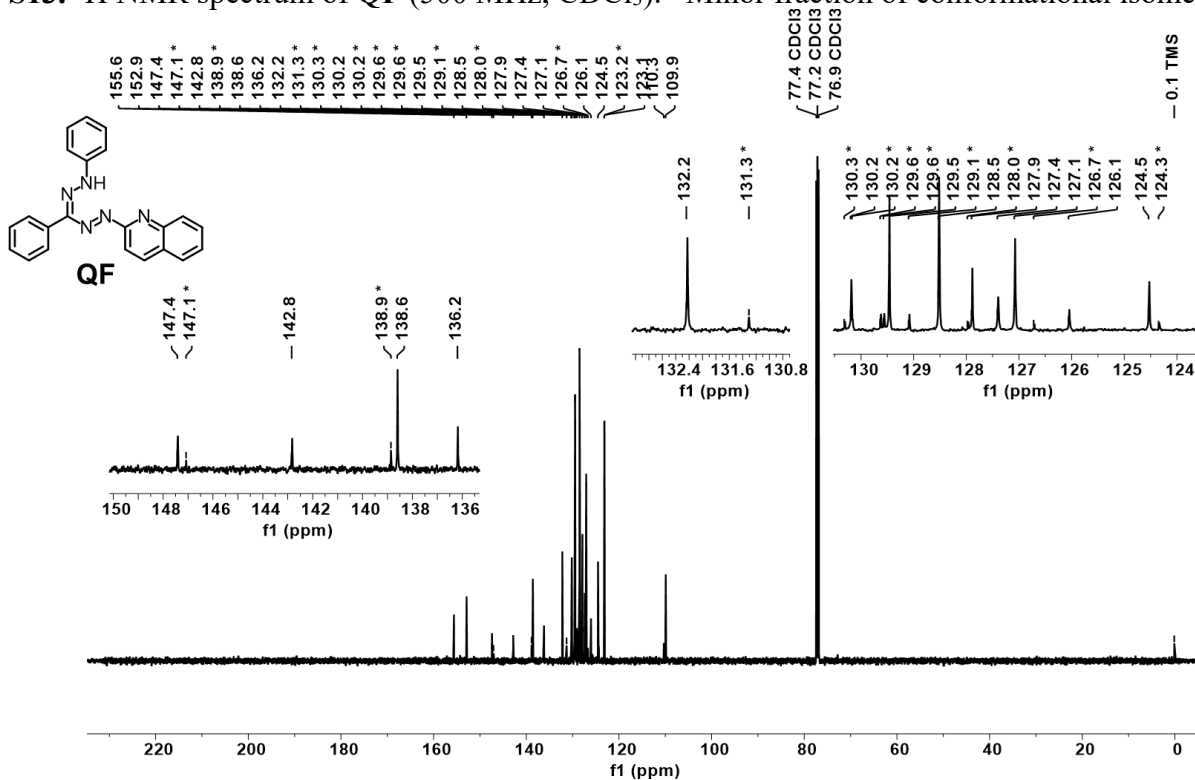
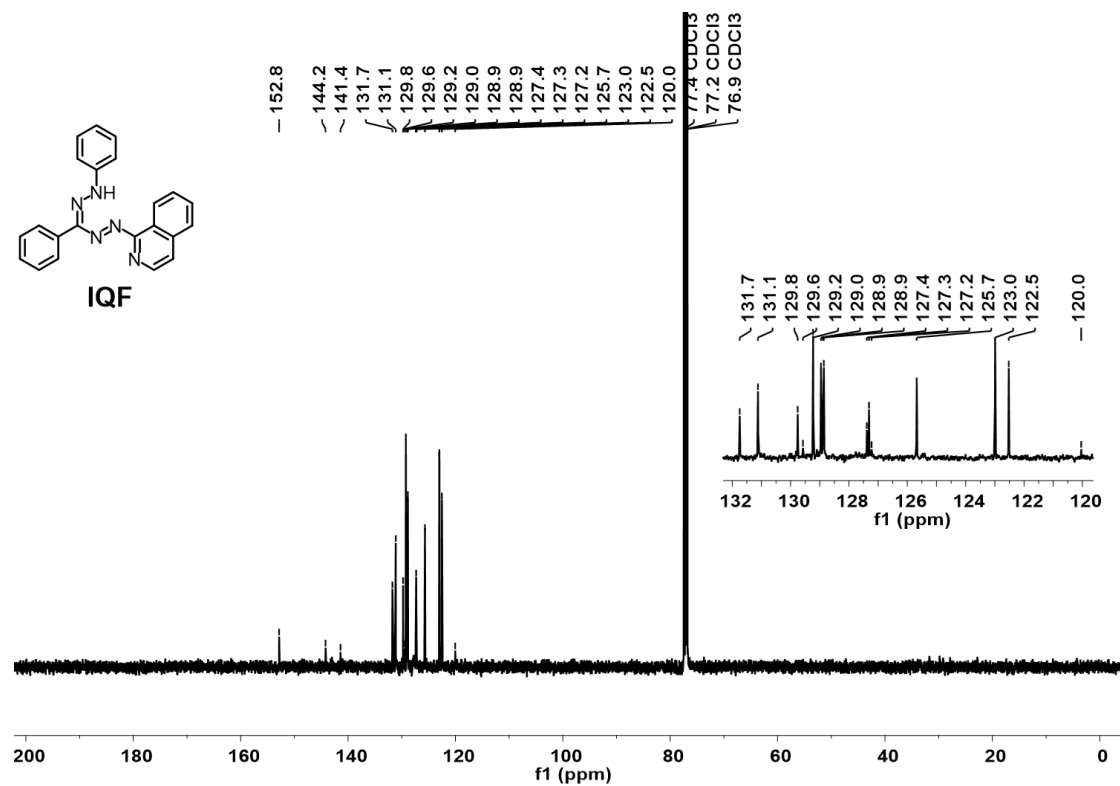
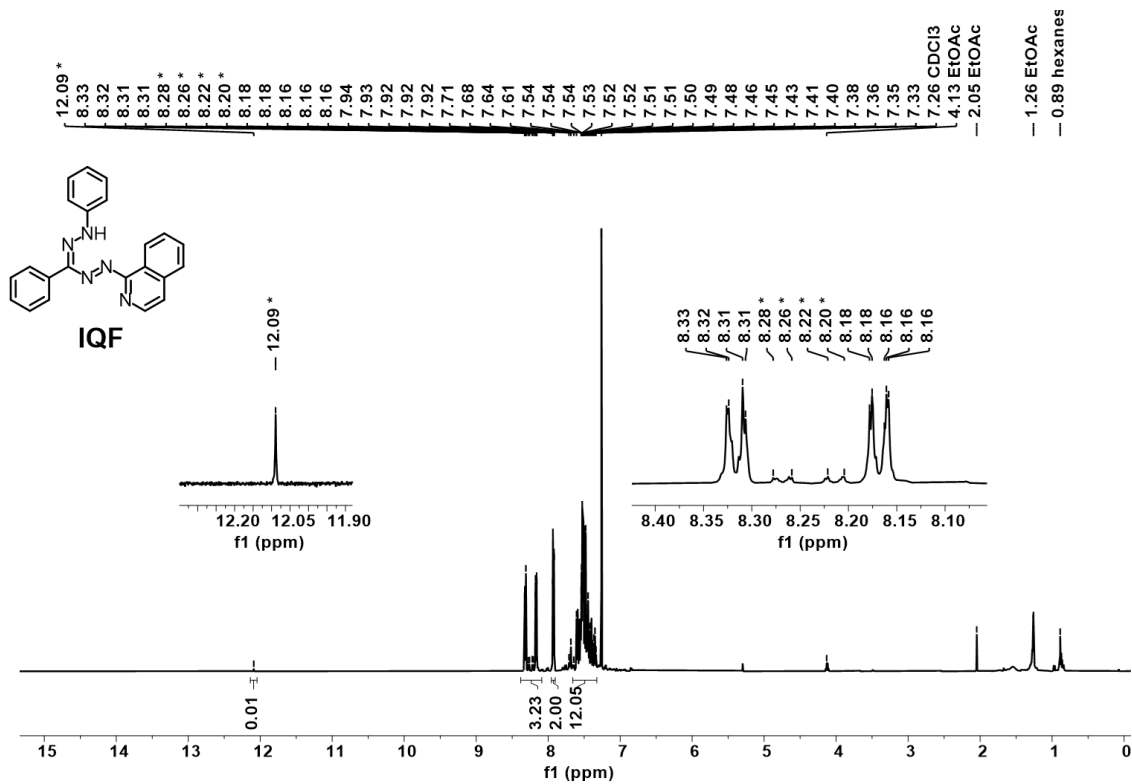


Figure S14.  $^{13}\text{C}$  NMR spectrum of QF (126 MHz,  $\text{CDCl}_3$ ). \*Minor fraction of conformational isomer.



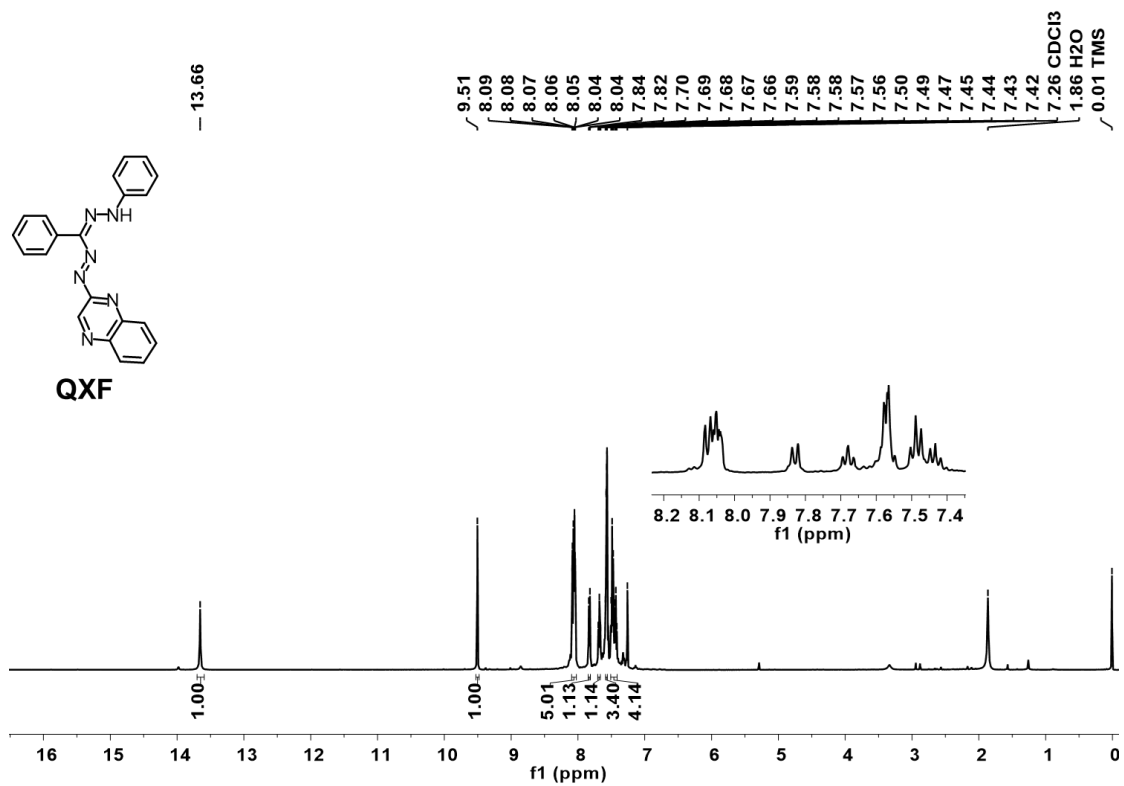


Figure S17. <sup>1</sup>H NMR spectrum of QXF (500 MHz, CDCl<sub>3</sub>).

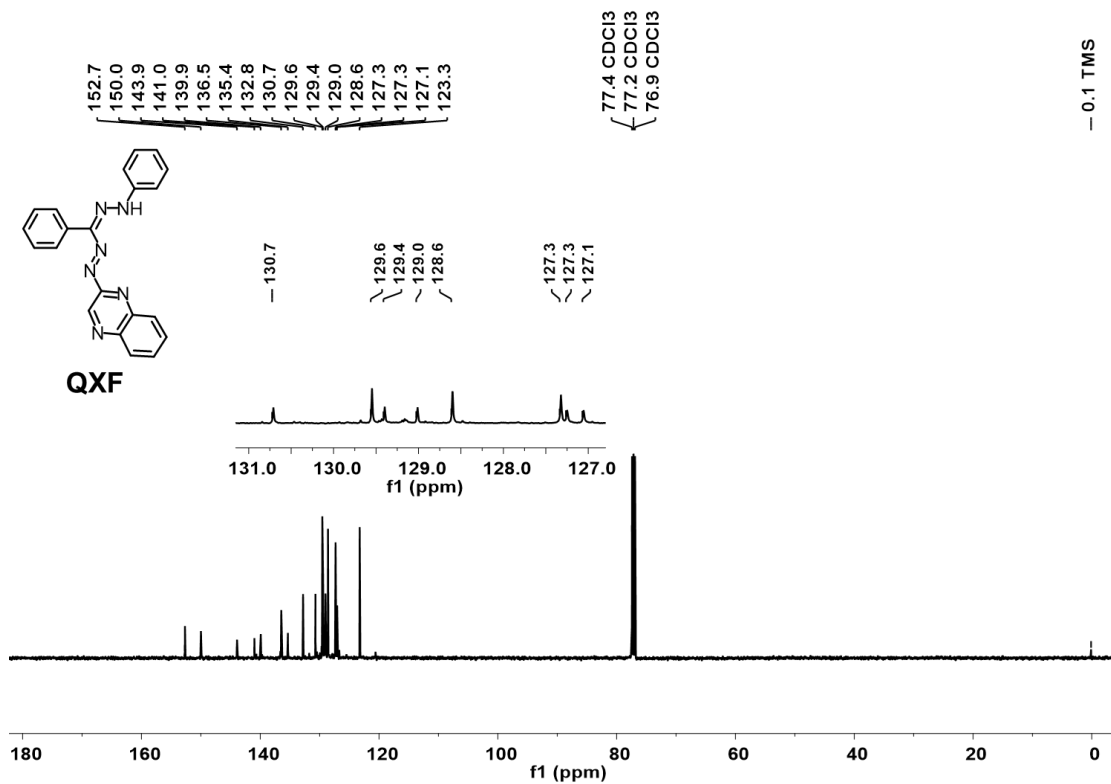


Figure S18. <sup>13</sup>C NMR spectrum of QXF (126 MHz, CDCl<sub>3</sub>).

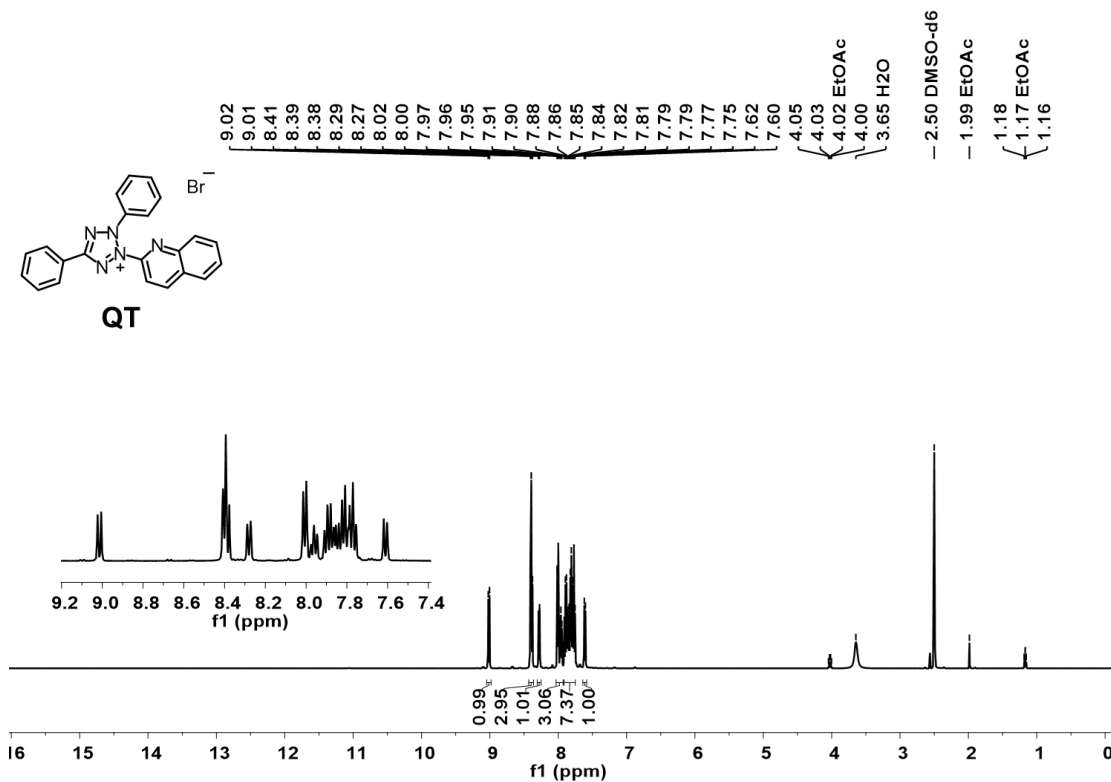


Figure S19. <sup>1</sup>H NMR spectrum of QT (500 MHz, DMSO-*d*<sub>6</sub>).

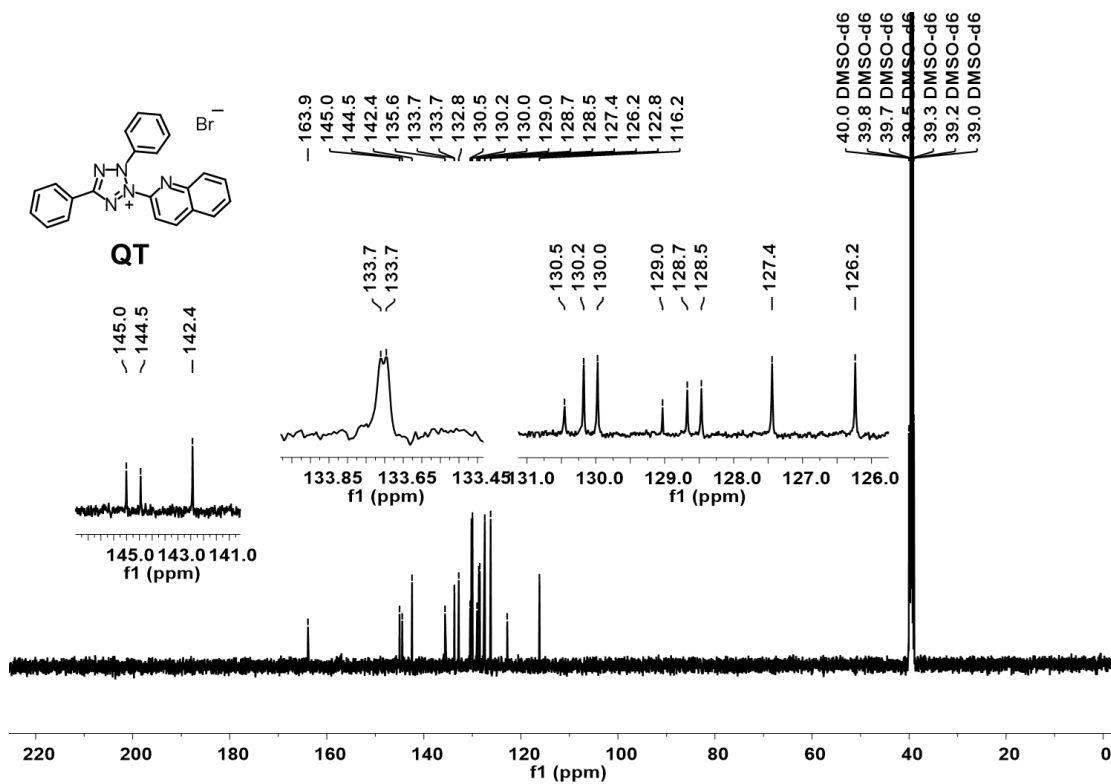
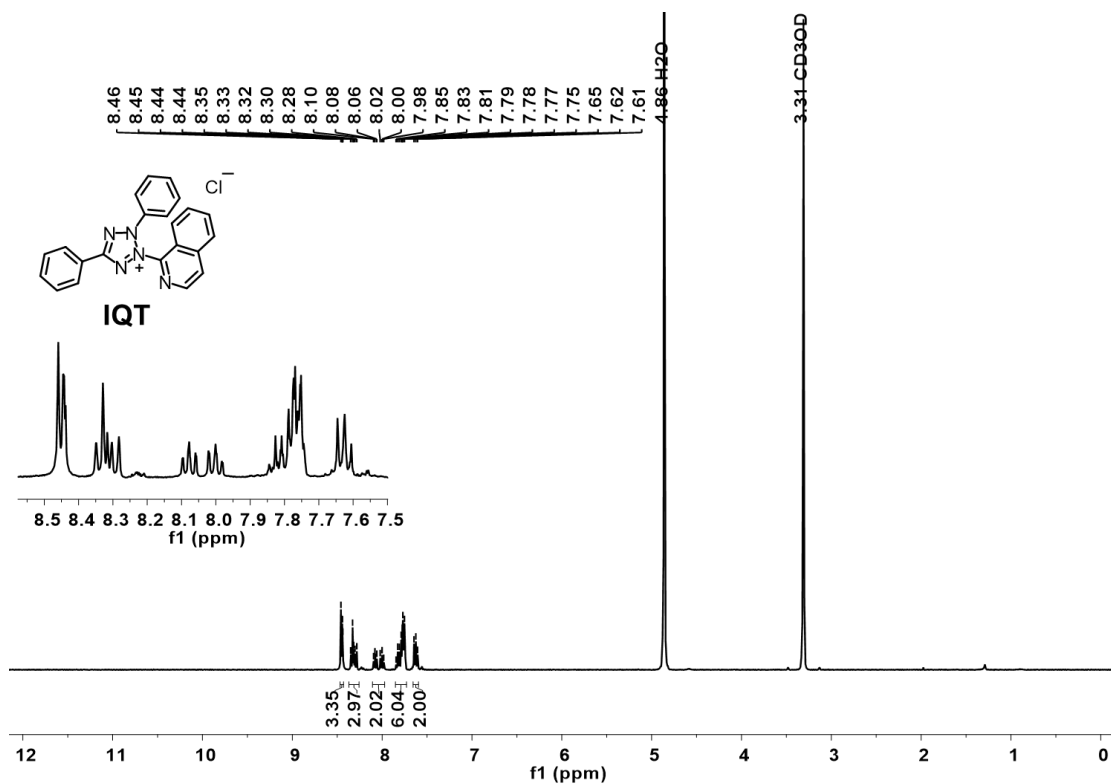
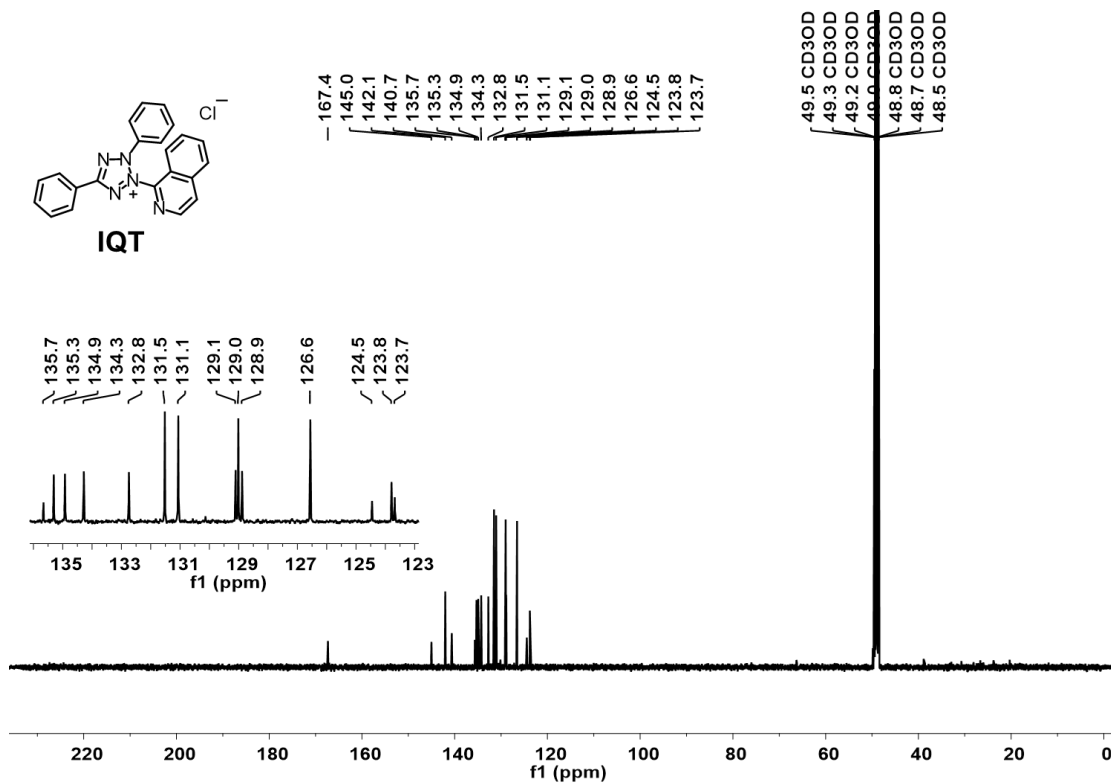


Figure S20. <sup>13</sup>C NMR spectrum of QT (126 MHz, DMSO-*d*<sub>6</sub>).



**Figure S21.**  $^1\text{H}$  NMR spectrum of IQT (500 MHz,  $\text{CD}_3\text{OD}$ ).



**Figure S22.**  $^{13}\text{C}$  NMR spectrum of IQT (126 MHz,  $\text{CD}_3\text{OD}$ ).



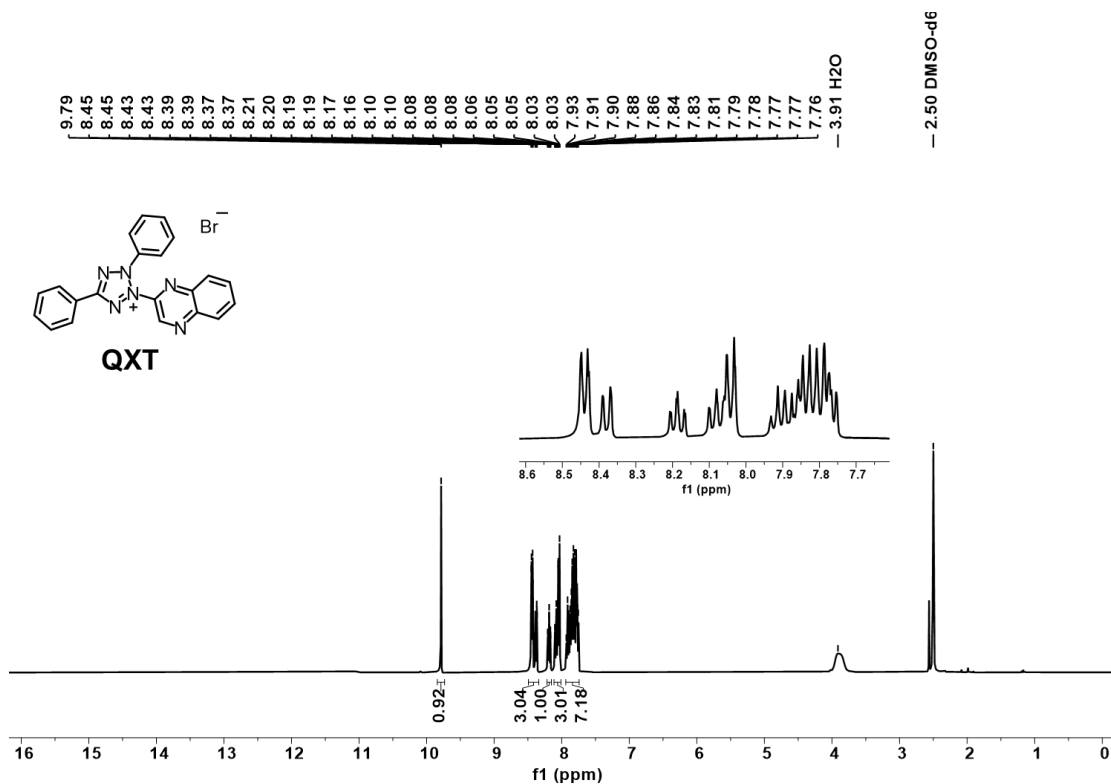


**Figure S23.** <sup>1</sup>H NMR spectrum of QXT (400 MHz, DMSO-*d*<sub>6</sub>).

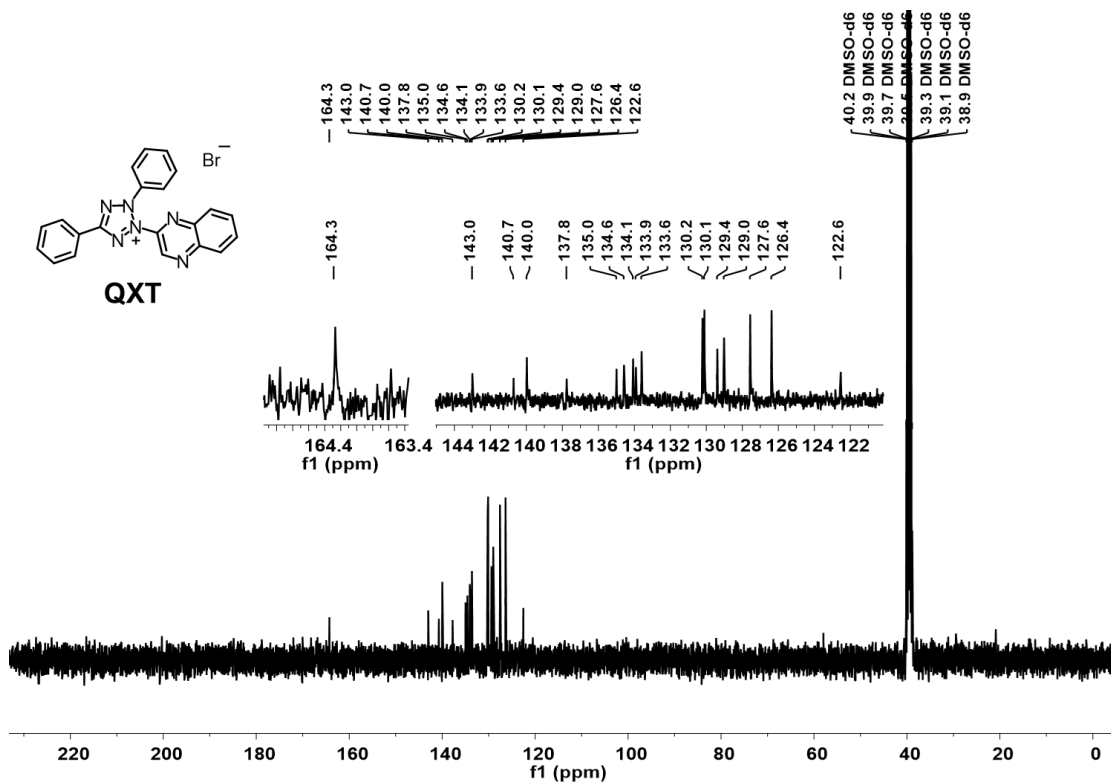


**Figure S24.** <sup>13</sup>C NMR spectrum of QXT (101 MHz, DMSO-*d*<sub>6</sub>).

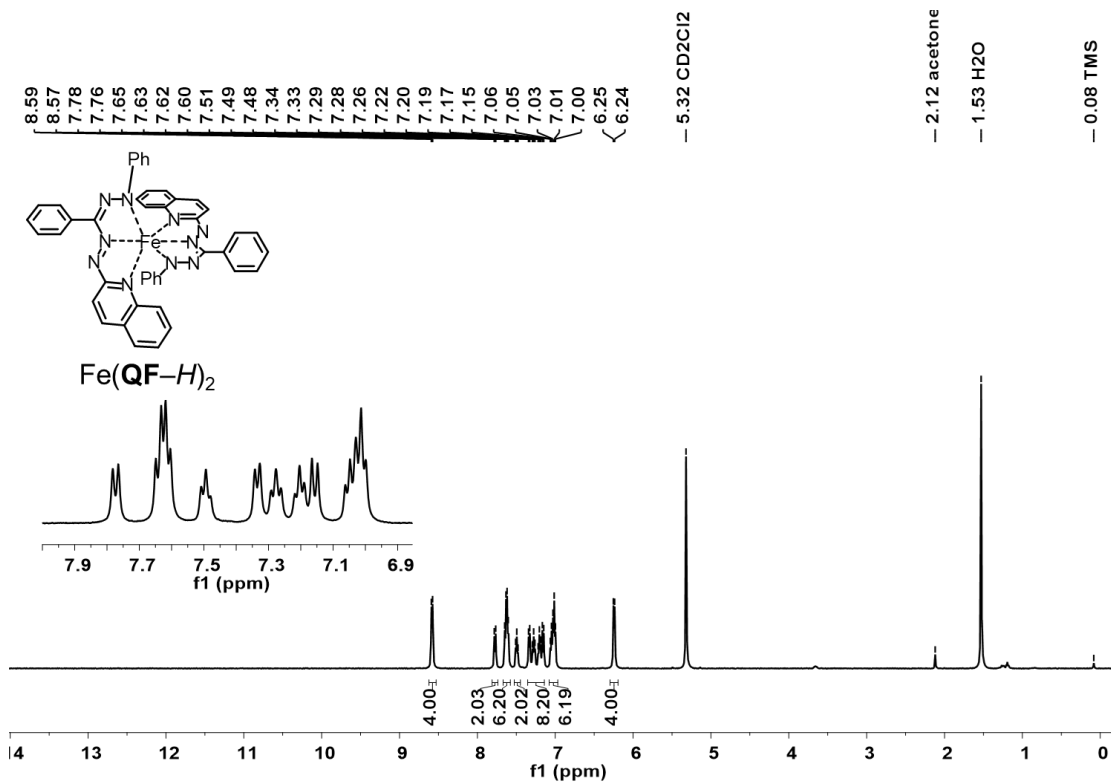


**Figure S25.** <sup>1</sup>H NMR spectrum of  $\text{Fe}(\text{QF-H})_2$  (500 MHz,  $\text{CD}_2\text{Cl}_2$ ).

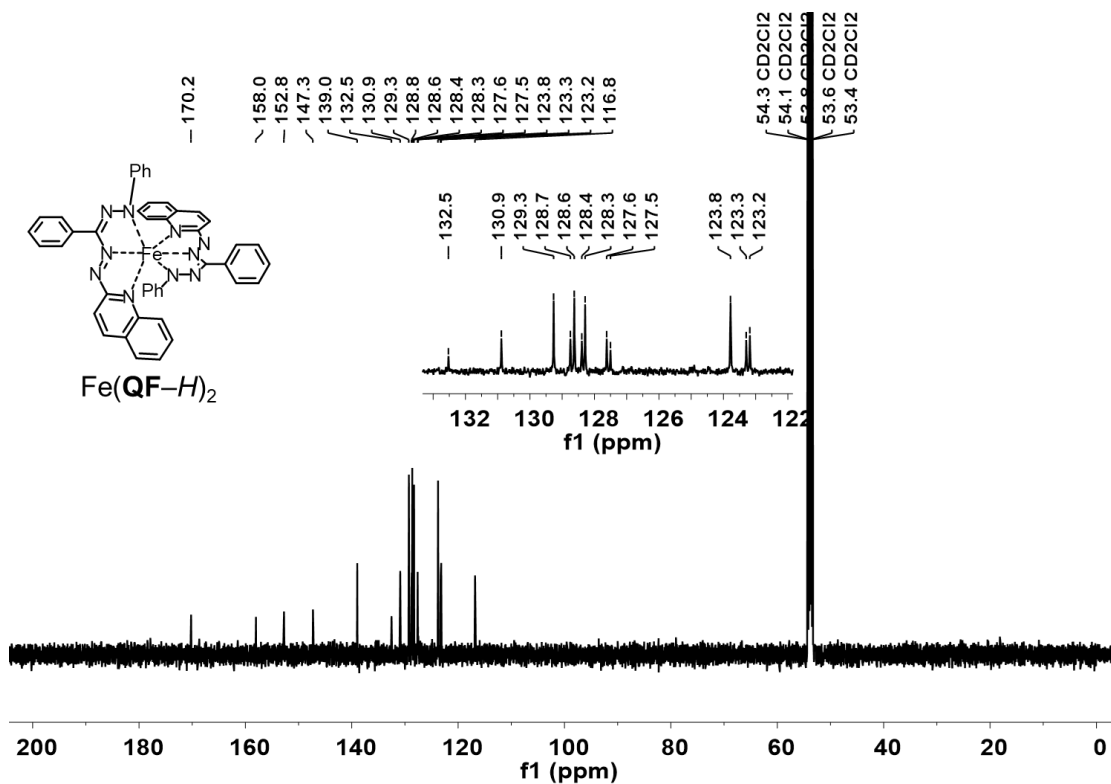


**Figure S26.** <sup>13</sup>C NMR spectrum of  $\text{Fe}(\text{QF-H})_2$  (126 MHz,  $\text{CD}_2\text{Cl}_2$ ).